

Cite this: *Sustainable Food Technol.*,
2023, 1, 738

Preparation and characterization of indicator films from chitosan/polyvinyl alcohol incorporated *Stachytarpheta jamaicensis* anthocyanins for monitoring chicken meat freshness

Yamanappagouda Amaregouda and Kantharaju Kamanna *

In this study, a novel multifunctional intelligent/active packaging material fabricated by immobilizing *Stachytarpheta jamaicensis* extracted (SJE) anthocyanins in a polymer matrix consisting of chitosan (CS) and polyvinyl alcohol (PVA) is described. The addition of SJE enhanced the tensile strength, barrier, and antioxidant activity of the films, and by increasing the SJE content, the tensile strength of the film reached $38.79 \pm 3.52\%$, and antioxidant activity was found to be $81.72 \pm 2.73\%$. The minimum oxygen permeability was $3.185 \pm 0.532 \times 10^{-6}$ (cc m⁻¹ 24 h atm), and the minimum water vapor permeability was 18.39 ± 0.18 g m⁻¹ h⁻¹. The UV-vis light transmittance and elongation at break were reduced when different contents of SJE were incorporated into the CS/PVA (CP) matrix. The smooth SEM images revealed that the miscibility and compatibility of the CP matrix with SJE anthocyanins were tolerable. The color of the film changed from pink to dark yellow when pH increased from 1 to 13. TGA profile indicated that the addition of SJE to CP significantly enhanced the thermal stability of the film. The prepared composite film changed color from pink to dark yellow when the estimated volatile base nitrogen content in the meat was 21.71 ± 0.59 mg/100 g. Hence, the prepared film with SJE can be used for the chicken meat packaging in real-time freshness monitoring at room temperature.

Received 23rd June 2023
Accepted 28th June 2023

DOI: 10.1039/d3fb00095h

rsc.li/susfoodtech

Sustainability spotlight

Present work employed natural *Stachytarpheta jamaicensis* extracted (SJE) anthocyanins into biodegradable natural and synthetic polymer consisting of chitosan (CS) and polyvinyl alcohol (PVA). The addition of SJE enhanced the overall physicochemical and bioactivity of the composite films prepared. Interestingly color of the film changed from pink to dark yellow when pH increased from 1 to 13. Hence, the prepared film with SJE can be used for the chicken meat packaging in real-time freshness monitor at room temperature. The material prepared is not harmful to the environment, and the prepared film is useful for monitoring the freshness of the chicken and the material is biodegradable.

Introduction

The new generation of active and smart food packaging materials with improved functional qualities has recently attracted the attention of polymer chemists.¹ The antioxidant and antimicrobial properties of additives included in the active packaging materials help food maintain its chemical or microbiological stability.² Time, color variation, and temperature are the most important parameters used to assess packaging material quality, which may be utilized to signal food freshness or the presence of gases and can perform functions of intelligent packaging.³ Since pH variation and food decomposition are typically closely related, visual indicator films can provide clear information through observable color changes.⁴

Thus, it is practical to assess the food freshness by identifying any variation in its pH values, which may be visibly shown using pH-sensing dyes.⁵ Due to adaptable construction and readily recognizable visual color fluctuation, pH-sensing indicators have recently attracted researchers in the field of food packaging and freshness monitoring.⁶ Various packaging films have already been established for shrimp, pig, and milk quality monitoring and pH-sensing indicators.⁷

Anthocyanins incorporated into polymer matrix have emerged as promising molecules for natural pigments and colorimetric indicators, and their antioxidant properties are well documented.⁸ Natural anthocyanins are isolated from a variety of fruits, flowers, and vegetables, as demonstrated previously.⁹ Anthocyanins can be employed as environmental sensors owing to their visual absorption spectrum and varied color with pH, temperature, and the presence of certain gases in the air.¹⁰ In this study, we have selected unreported Verbenaceae family species *Stachytarpheta jamaicensis*, also known as

School of Basic Sciences, Department of Chemistry, Rani Channamma University, Vidyanagama, P-B, NH-4, Belagavi 591156, Karnataka, India. E-mail: kk@rcub.ac.in; Fax: +91-831-2565240; Tel: +91-831-2565203



Gervao, Brazilian tea, verbena cimarrona, rooster comb, or blue porter weed.^{11,12} It is a significant plant with important medicinal and nutritional properties.¹³ Traditional and folk medicine systems use *S. jamaicensis* for its wide range of therapeutic characteristics, which include treatment for many ailments that have been well-reported.¹⁴ From studies on anthocyanins extracted from blue flowers of *Stachytarpheta jamaicensis* (SJE), researchers have discovered a wide range of colors from pink to yellow in their aqueous extract.¹⁵ Furthermore, the same authors investigated SJE's color intensity and total anthocyanin and total phenolic contents.

Numerous non-toxic and biodegradable polymers derived from synthetic or natural sources, including pectin, agar, chitosan, and polymer-immobilized natural anthocyanins, have been well documented.⁷ Chitosan (CS) is one of the natural polymers, and it is a common polysaccharide found in sea animals.¹⁶ Chitosan is used in a variety of sectors, including biomaterials, separation, and biosensors, because of its capacity to form films with antibacterial properties and biodegradability. Food packets containing CS kept food fresh without a freezer for a longer period, and biodegrading prevented future soil contamination. However, the fast dissolution in acidic solution and lack of flexibility of the CS films are its drawbacks.¹⁷ Polyvinyl alcohol (PVA), another exceptional synthetic polymer, also showed numerous qualities in food packaging, including a high degree of hydrophilicity, outstanding chemical stability, biodegradability, and film-formation abilities.^{18–21} Researchers have extensively studied PVA blended chitosan films for structural, antibacterial, and fruit preservation properties.²² Additionally, PVA/CS film showed good antibacterial activity, but it also enhanced mechanical properties. Food packaging films made of PVA or CS alone exhibited poor mechanical properties and were not fit for use as food packaging materials.²³ Recent research trends show multifunctional composite films with improved mechanical, antioxidant, antibacterial, and barrier capabilities and polymer-doped natural anthocyanins as self-indicators in food packaging and other material applications. Some of the noted reported examples are; CS/PVA composite films developed from bio-waste orange peel in food packaging.²⁴ Real-time monitoring of fish freshness was achieved by the fabrication of intelligent/active films based on CS/PVA matrices containing *Jacaranda cuspidifolia* anthocyanins.²⁵ Anthocyanins from *Brassica oleracea* (red cabbage) have been used in CS/PVA films as real time–temperature indicator in intelligent food packaging.²⁶ Intelligent pH indicator films with enhanced optical and thermal properties based CS/PVA with novel Xanthylum dye have been fabricated.²⁷ Rutin-induced CS/PVA bioactive films for food packaging applications, physical, chemical, and functional properties,²⁸ and many more active and intelligent natural extract doped films were reported in the literature. In the present work, we aimed to develop smart packaging materials by adding natural anthocyanins extracted from *Stachytarpheta jamaicensis* (SJE) into CS/PVA polymer blend for the first time. The effects of SJE content on the structural, physical, antioxidant, cell viability, and pH sensitive properties of prepared composite films were determined. The

studies revealed that the prepared films can be applied to monitor the freshness of chicken meat.

Materials and methods

Materials and reagents

The fresh chicken meat was purchased from the local meat market. Chitosan (CS, MW: 190–310 kDa, 95% deacetylation) was purchased from Loba, India. Polyvinyl alcohol (PVA, MW: 25 000 g mol⁻¹, degree of alcoholysis 98%) was purchased from HIMEDIA India. *Stachytarpheta jamaicensis* flowers were collected from the forest area near Rani Channamma University, Belagavi (Karnataka, India). The following chemicals were purchased from Sigma-Aldrich, India: 2,2-diphenyl-1-picrylhydrazyl (DPPH), gallic acid, rutin, cyanidin-3-glucoside, magnesium oxide (MgO), methyl red (C₁₅H₁₅N₃O₂), methylene blue (C₁₆H₁₈N₃ClS), boric acid (H₃BO₃), and hydrochloric acid (HCl).

Extraction of *Stachytarpheta jamaicensis* flower anthocyanins

Stachytarpheta jamaicensis anthocyanins were extracted using our previously reported procedure.²⁵

Determination of total anthocyanins content

UV-vis spectrophotometer was used for the determination of total anthocyanins of extracted crude powder. Briefly, 10 mL of DI water was used to dissolve 10 mg of crude powder,²⁹ and 1 mL of the solution was combined with 9 mL of 0.2 M potassium chloride solution (pH 1.0). A pH 4.5 buffer containing 0.4 M sodium acetate was used for dilution. At 510 nm, the absorbance of each solution was determined. The following eqn (1) was used to determine the total anthocyanin content.

$$\text{Anthocyanin content (mg L}^{-1}\text{)} = (A \times M_w \times DF \times 1000)/(\epsilon \times L) \quad (1)$$

where $A = A_{510}(\text{pH } 1.0) - A_{510}(\text{pH } 4.5)$, M_w = the molecular weight of anthocyanins (433.2 g mol⁻¹), DF = the dilution factor, ϵ = the extinction coefficient (31 600 L cm⁻¹ mol⁻¹) and L = the path length (1 cm).

Fabrication of films

1 g of chitosan (CS) was taken in 100 mL of 1% aq. acetic acid, and continuously stirred under a magnetic stirrer until the solution becomes clear. Subsequently, a PVA solution was prepared by 0.5 g of PVA in 50 mL of hot distilled water under a magnetic stirrer. The final solution was prepared by mixing CS and PVA solution at a ratio of 1:0.5 (w/w) under magnetic stirring for about 10 min. The resulting solution was cast on a dried Petri dish and allowed to dry for 5 h at 50 °C in a hot air oven. The resulting film was named CP (CS/PVA) and used as a control. To consider the effect of anthocyanins on CS/PVA films, different concentrations of SJE (0.33, 0.66, 1.00, 1.33, and 1.66 wt%) were added to the CS/PVA solution, as prepared above, and the samples were denoted as CP-SJE-I, CP-SJE-II, CP-SJE-III, CP-SJE-IV, and CP-SJE-V, respectively. The resultant



solutions were poured into pre-cleaned and pre-dried glass plates and then dried at 50 °C for 8 h. After that, the films were peeled off from the glass plates and stored at 25 ± 1 °C with relative humidity (RH) of $55 \pm 1\%$ for 48 h.³

Estimation of total phenolic and flavonoid contents

The Folin-reagent Ciocalteu's method was used to calculate total phenolic content (TPC). Gallic acid equivalents (GAE) per g were used to express the results in mg of the material. The reported method was used to determine the total flavonoid content (TFC) and was performed three times for the data collection.³⁰ The average of three replicates was used to express the sample results in mg rutin equivalents (RE) per g.³⁰

Techniques and characterization

A UV-vis spectrophotometer was used to measure the extracted anthocyanins (Shimadzu, UV-1800, USA) in the range of 400–800 nm with varied pH 1.0–13.0. Briefly, the sample was prepared by weighing 2 mg of the dried extract soaked in 20 mL of buffer solution (pH 1–13) for about 30 min in order to determine the SJE pH sensitivity. A digital camera was used to capture the color of the solution, and the absorption spectra were collected from 400 to 800 nm.³ The pH-responsive properties of the prepared films were assessed using a modified procedure of a previously reported method. The film samples (20 × 20 mm) were placed on a Petri dish with various pH (1–14) solutions (5 mL), and the pictures were captured in a digital camera for visible color change of the films.³¹ ATR-FTIR spectra were collected for the prepared films using Fourier-transform infrared spectroscopy (Thermo-Scientific, Nicolet iZ10) over the range of 4000 to 600 cm^{-1} at a resolution of 4 cm^{-1} . The samples were tested in the ATR total reflection mode directly. The surface morphology of the prepared films was examined by SEM (VEGA3, TESCAN, Czech Republic). A thin palladium/platinum conductive coating was applied to the sample before processing. Sputter coating was employed to generate the layer, and a secondary electron detector with a 30 kV accelerating voltage was used for film surface investigation. The thickness of the prepared film was measured by a micrometer (Mitutoyo, Japan) with precision of 0.001 mm in a universal testing machine. The mechanical properties of the prepared films were studied according to the ASTM D88291 (DAK System, 7200 Series, India) at ambient temperature. A film sample of uniform thickness (25 × 100 mm) was introduced with a grip partition of 5 cm and stretched at a crosshead speed of 1 mm min^{-1} . The impact of added anthocyanins on the thermal decomposition of polymer matrix films is investigated using TGA. A thermogravimetric analyzer (TA-SDT650 Instruments, USA) was used to obtain sample thermograms in the temperature range of 25 °C to 600 °C at a rate of 10 °C min^{-1} increase. The transmittance, opacity, and transparency of the prepared film samples were studied using a UV-vis spectrophotometer (Shimadzu, UV-1800, USA). Briefly, the film sample (40 × 10 mm) with uniform thickness was placed in a UV cell, and data were recorded in the 250–800 nm range and air as a standard reference. The opacity at 500 nm and transparency at 600 nm were calculated using

eqn (2) and (3), respectively. The experiments were performed in triplicates, and averaged data were used for estimation.³²

$$\text{Opacity}_{500} = \frac{\text{Abs}}{\chi} \quad (2)$$

$$\text{Transparency}_{600} = \frac{-\log(\% T)}{\chi} \quad (3)$$

where Abs – the absorbance value at 500 nm, % *T* – the transmittance percentage at 600 nm, and χ – the film thickness (mm).

Barrier, biological and packaging properties

Moisture content. The moisture content of the prepared films was determined by drying the film sample at 110 °C to a constant weight.³³

$$\text{Moisture content (\%)} = \frac{M_i - M_t}{M_i} \times 100 \quad (4)$$

where M_i and M_t are the initial and final mass of the film sample, respectively.

Water vapor transmission rate (WVTR). In order to conduct this test, 10 mL of deionized water was placed into a sample glass bottle with a 30 mm inside diameter. Teflon tape was used and tightly wrapped with films around the bottle mouth. The weight of the bottle was measured and then placed in an oven at 40 °C for 24 h. The bottle was taken out from the oven after 24 h and weighed once again. According to the following equation,³⁴ the WVTR was calculated for the film:

$$\text{WVTR} = [W_i - W_t/A] \times T \text{ (g m}^{-2} \text{ h}^{-1}) \quad (5)$$

where *A* = area of the circular mouth of the glass bottle; *T* = 24 h; W_i = initial weight of the glass bottle; W_t = final weight of the glass bottle.

Water solubility. Water solubility properties were measured by adopting the outlined procedure³⁵ with a minor change of the method. Briefly, water solubility (WS) of the pH-sensitive indicator films prepared was assessed using sample film (20 × 30 mm), weighed and dried for 24 h at 100 °C in an oven (M_i). Each sample film was placed in 50 mL of ultrapure water for 24 h at room temperature. The film was then taken out from the water, again dried for 24 h at 100 °C, and weighed to get the final dry weight (M_f). The following equation was used to assess the water solubility of the film:

$$\text{WS (\%)} = \frac{M_i - M_f}{M_i} \times 100 \quad (6)$$

Oxygen permeability. The oxygen permeability (OP) of prepared films was determined by employing a reported protocol with slight modification.³⁶ Briefly, a bottle (100 mL), with a strip covering and sealed mouth by the prepared film (30 × 30 mm), was kept in a desiccator at room temperature. Every day, the weight of the bottle was recorded for up to three days. A linear regression analysis of the weight change vs. time ($R^2 > 0.99$) was used to calculate the slope of each line utilizing eqn



(7) and (8). The total OPTR (Oxygen Permeability Transmission Rate) and OP were determined from a reported procedure.³⁶

$$\text{OPTR} = \frac{\text{slope}}{\text{film area}} \quad (7)$$

$$\text{OP} = \frac{\text{OPTR} \times L}{\Delta P} \quad (8)$$

ΔP = difference in partial vapor pressure between pure water and dry atmosphere (0.02308 atm at 25 °C), L represents average film thickness. The measurements were determined in triplicate for each sample.

Release of anthocyanins from the film

The food simulants such as distilled water, 50% ethanol, and 3% acetic acid mimic aqueous food, alcoholic beverages, and acidic foods, respectively. The release of the loaded anthocyanin content from the film sample into food is assessed (Shimadzu, UV-1800, USA). Briefly, a film (20 × 20 mm size) was kept in a beaker containing food simulants and swirled for 6 h at room temperature. Then, UV-vis absorbance at 520 nm was measured for each sample solution, and using the cyanidin-3-glucoside standard curve, the concentration of the anthocyanins released was calculated (0, 0.1, 0.3, 0.5, 0.7, and 0.9 g mL⁻¹).³⁷

Antioxidant activity

The antioxidant activities of the prepared films were evaluated using DPPH radical scavenging assays. In order to conduct this investigation, 2 mL of methanolic DPPH (0.39 g mL⁻¹) and 1 mL of the film sample solution (0, 20, 40, 60, 80, and 100 g mL⁻¹) were carefully mixed, and incubated at 23 ± 2 °C for 30 min, followed UV-vis absorbance at 517 nm. The tests were carried out for each sample three times, and the mean SD values were used to express the results. The DPPH inhibition test was calculated using eqn (8), and ascorbic acid was used as a standard reference (AA).¹⁸

$$\text{DPPH assay} = \frac{A_{\text{DPPH}} - A_{\text{sample}}}{A_{\text{DPPH}}} \times 100 \quad (9)$$

Cell viability assay

The cell viability of the prepared films was tested using MTT (3-(4,5-dimethylthiazol-2-yl)-2,5-diphenyl tetrazolium bromide) assay using a reported method.²⁵

Application of prepared CP-SJE-V film for indicating the freshness of the chicken meat

To indicate the freshness of the chicken meat, a rectangular shaped CP-SJE-V film sample was placed in the headspace of a Petri dish containing 30 g of fresh chicken meat.³⁸ Then, the Petri dish was stored at ambient temperature and monitored for about 48 h. The color change of the film CP-SJE-V was recorded by digital camera photograph. Afterwards, 10 g of the chicken meat sample was homogenized in 100 mL of distilled water and transferred to a Kjeldahl distillation apparatus (K9860, Jinan

Hanon, China) containing 1 g of MgO to measure homogenate total volatile basic nitrogen (TVB-N) concentration. The distillate was collected and titrated with 0.01 mol L⁻¹ of HCl solution in a flask containing 10 mL of 2% boric acid solution.

Statistical analysis

The graphical data of the several sample properties obtained were examined for mean and standard deviation using Origin software, and a one-way analysis of variance (ANOVA) was performed on data and $P < 0.05$ regarded as a significant value.

Result and discussion

Total phenolic content, total flavonoid content, and total anthocyanin content

Researchers have reported that most of the potent plant metabolites showed antioxidant activity due to the presence of polyphenolic compounds present in it. As a result, there should be a strong relationship between antioxidant activity and phenolic component concentration. Additionally, natural sources of phenolic and flavonoid levels of antioxidants may be utilized as strong indications.³⁰ The TPC and TFC of the extracted *Stachytarpheta jamaicensis* anthocyanins were found to be 299 mg GAE/100 g d.w. and 352 mg RE/100 g d.w., respectively. The concentration of the SJE anthocyanins was measured using the pH differential method, and SJE anthocyanins content was found to be 0.529 g mL⁻¹.

Color evaluation as a pH-sensing indicator, and pH-dependence of anthocyanins color

The color variation of the SJE solution in different pH buffer solutions was measured and is appended in Fig. 1. Remarkable color distinction is observed for SJE with pH ranges 1–4, 7, and 10–13 showing red, colorless, and yellow, respectively.³⁹ The impact of pH on the color change of the CP-SJE films is shown in Fig. 1 (below images). The maximum absorption peak of SJE solution shifted from 520 nm (acidic) to 607 nm (basic), as presented in Fig. 2. The color change and corresponding bathochromic shift in maximum absorption peak are mainly caused by the constituent chemical structure transformation present in the anthocyanins at different pH.

ATR-FTIR spectra of prepared films

Fig. 3 represents the characteristic ATR-FTIR spectra collected for CP, CP-SJE I, CP-SJE II, CP-SJE III, CP-SJE IV, and CP-SJE V. The control CP film showed absorption bands characteristic of both chitosan and PVA (OH at 3387 cm⁻¹, CH₂ at 2895 cm⁻¹, C=O (amide I-chitosan) at 1626 cm⁻¹, NH₂ overlaps C-N at about 1569 cm⁻¹, C-O at 1101 and 1083 cm⁻¹). The spectra of CP-SJE I, CP-SJE II, CP-SJE III, CP-SJE IV, and CP-SJE V show a clear decrease in the intensity of the band at 3389 cm⁻¹, attributed to the interaction among the functional groups of CS/PVA matrix and anthocyanin.²⁷ The results of FTIR analysis showed that anthocyanin adsorbed onto the CS/PVA matrix by physical interaction without



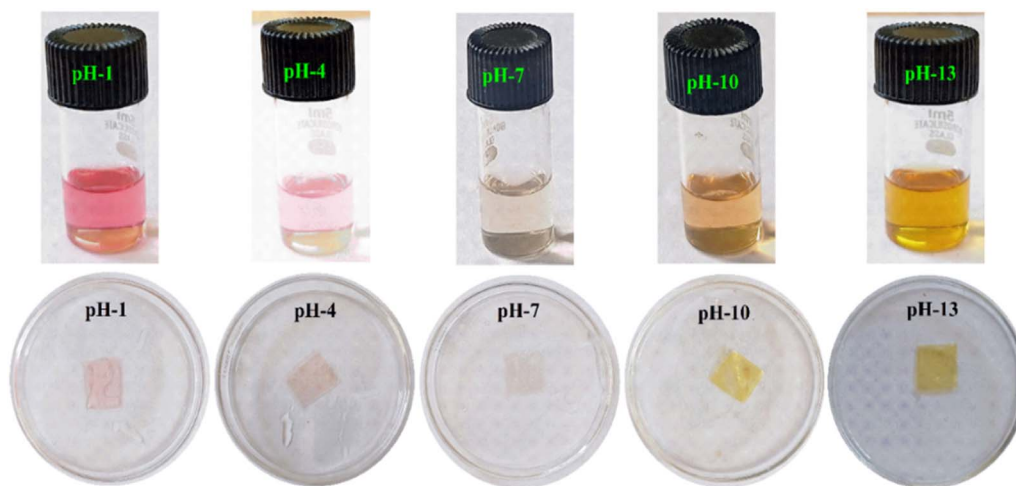


Fig. 1 Color response of the SJE anthocyanin solutions and pH response of CP-SJE-V film with different buffer solutions of pH 1–13.

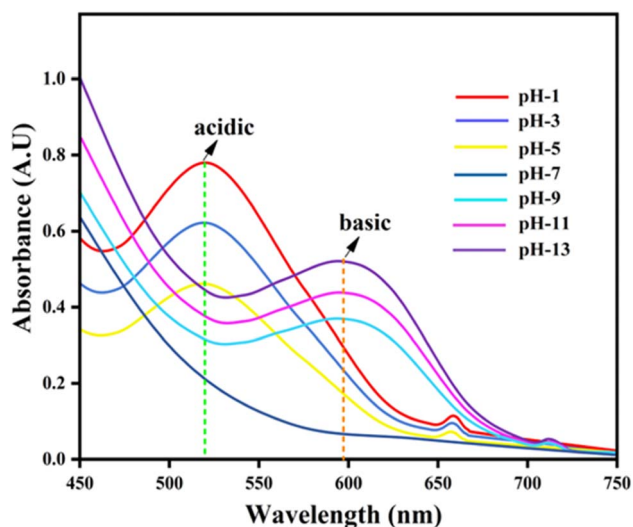


Fig. 2 UV-vis spectra of *Stachytarpheta jamaicensis* anthocyanins measured in various buffer solutions (pH 1–13).

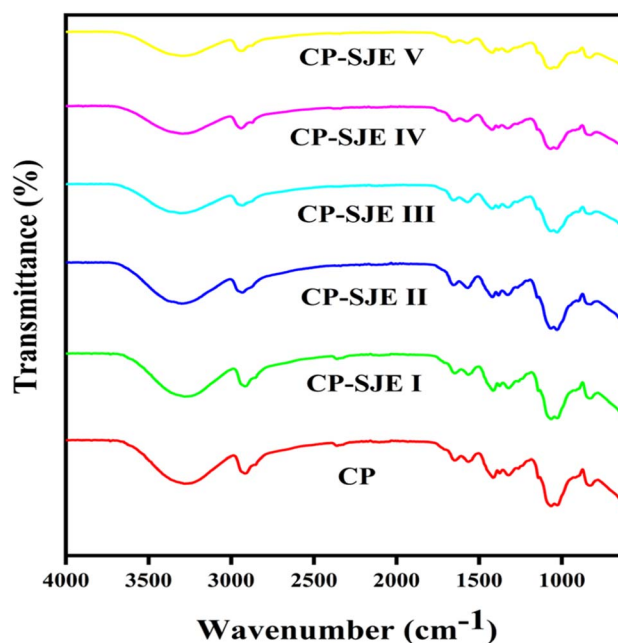


Fig. 3 FT-IR spectra of prepared CP and CP-SJE films.

changing the chemical structure of the CS/PVA matrix or forming a chemical interaction between them.

Thickness

The film thickness is an important parameter that directly affects the mechanical strength and barrier properties of the food packaging application.⁴⁰ The observed data is appended in Table 1, and shows film thickness increased from 30.31 to 44.61 μm with SJE amount increasing from 0 to 6 wt% from control CP film to CP-SJE-I, CP-SJE-II, CP-SJE-III, CP-SJE-IV, and CP-SJE-V, being significantly thicker ($p < 0.05$). This experimental data suggested that the thickness of the CP combined SJE films was affected by SJE content. The large amounts of SJE (0.33, 0.66, 1.00, 1.33, and 1.66 wt% on the CP matrix) could create more complex matrices based on anthocyanins on the CP surface, resulting in a relatively high thickness of the CP-SJE films.

Surface morphology of CP and CP-SJE films

The surface morphology of the CP and various % of CP-SJE prepared films were investigated by SEM. The surface morphology of each film is shown in Fig. 4. In general, the surface of the control CP film was uniform, smooth, and crack and bubble free morphology, indicating CS and PVA were homogeneously mixed, forming a good film texture.⁴¹ A few white spots presented on the surface of the CS-SJE blended films indicate some heterogeneity in the CP matrix when SJE is incorporated (Fig. 4). Thus, the intermolecular interactions formed between CS/PVA and SJE contents could contribute to the improvement of the barrier properties of CP-SJE films.



Table 1 Thickness, transparency, and opacity properties of the prepared films^a

| Sample | Thickness (μm) | Transparency at 600 nm | Opacity at 500 nm |
|------------|-----------------------------|------------------------|---------------------|
| CP | 30.31 ± 1.21^a | 73.19 ± 2.01^a | 1.3 ± 0.01^a |
| CP-SJE-I | 33.29 ± 1.32^b | 52.25 ± 1.93^b | 1.5 ± 0.05^{ab} |
| CP-SJE-II | 35.26 ± 2.00^c | 51.62 ± 2.62^{ac} | 1.9 ± 0.09^c |
| CP-SJE-III | 39.42 ± 1.29^d | 34.71 ± 2.58^c | 2.3 ± 0.03^b |
| CP-SJE-IV | 42.54 ± 2.11^{ab} | 29.39 ± 2.92^d | 2.7 ± 0.02^{ac} |
| CP-SJE-V | 44.61 ± 1.58^{ac} | 26.53 ± 3.00^{ad} | 3.1 ± 0.01^{ad} |

^a ^{a-d}Different letters represent statistical difference at $p < 0.05$, $n = 3$.

Optical property

Foods can deteriorate easily when they are exposed to UV-vis light. Thus, UV-vis light barrier property for food packaging films is crucial.²⁵ The visual appearance of the CP-SJE film is shown in Fig. 5a. As presented in Fig. 5b, CP-SJE films had remarkably lower UV-vis light transmittance in comparison to the control CP film. This indicated that CP-SJE films possessed strong UV-vis light barrier properties than the control CP film. Further, the UV-vis light barrier properties of the CP-SJE films increased with increasing concentration of the SJE. This optical property of the prepared CP-SJE films could effectively protect food against UV radiation. Transmittance at 600 nm was used to assess the transparency and opacity value of the films, and the

findings are displayed in Table 1. At 600 nm, the transparency of SJE-induced CP-SJE films was reduced. The opaqueness of the developed films and restriction of light passage or light scattering by the SJE distributed in the CP matrix clearly established the SJE plays a vital role in blocking both UV and visible light. As a result, the SJE-induced films showed outstanding UV light barrier performance and may be employed for food packaging for oxidation-prone materials storage.

Mechanical property

Mechanical properties of the film reflect the ability of packaging to maintain good integrity and sustainability in the food supply chain.⁴² The mechanical properties of the prepared films,

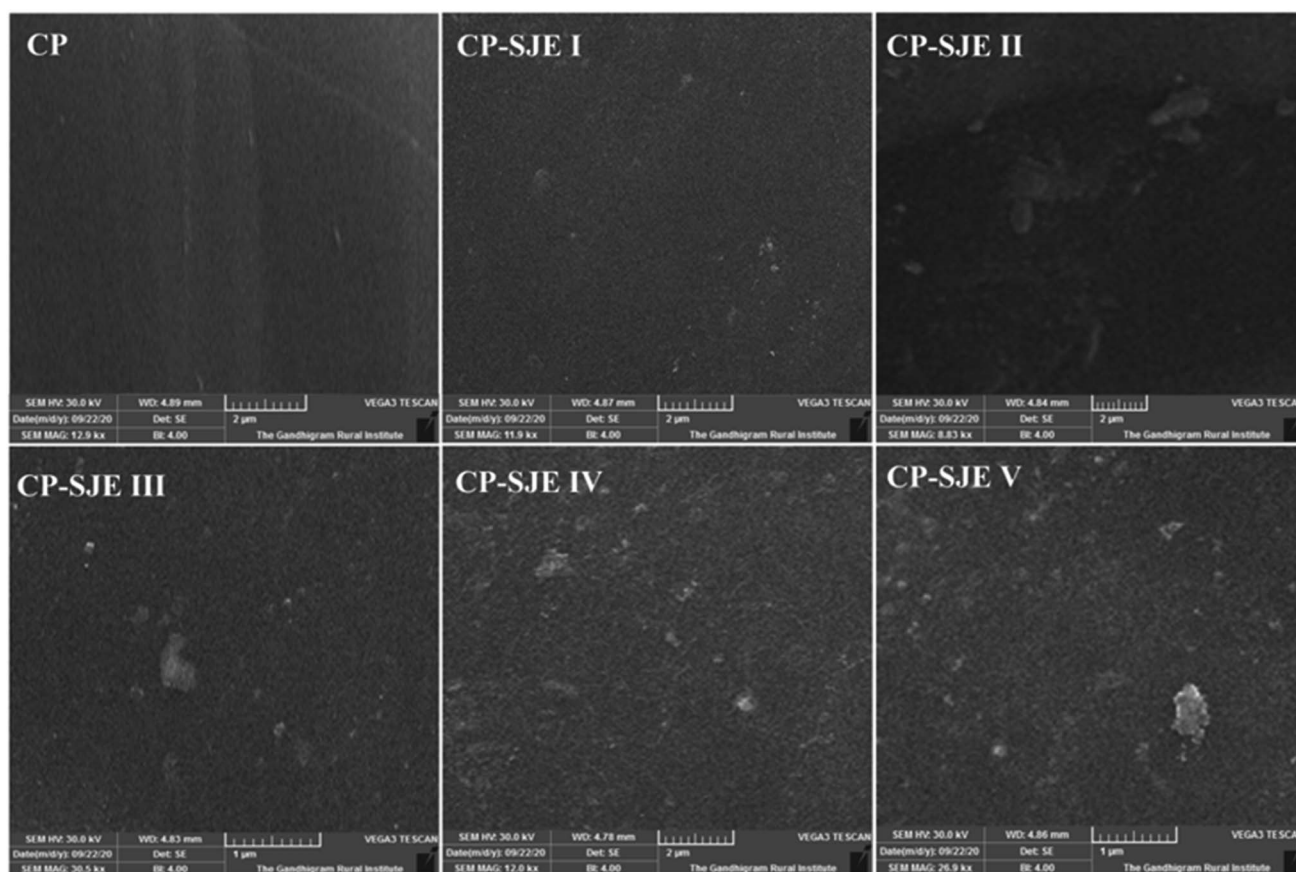


Fig. 4 Surface morphology of prepared CP and CP-SJE films.



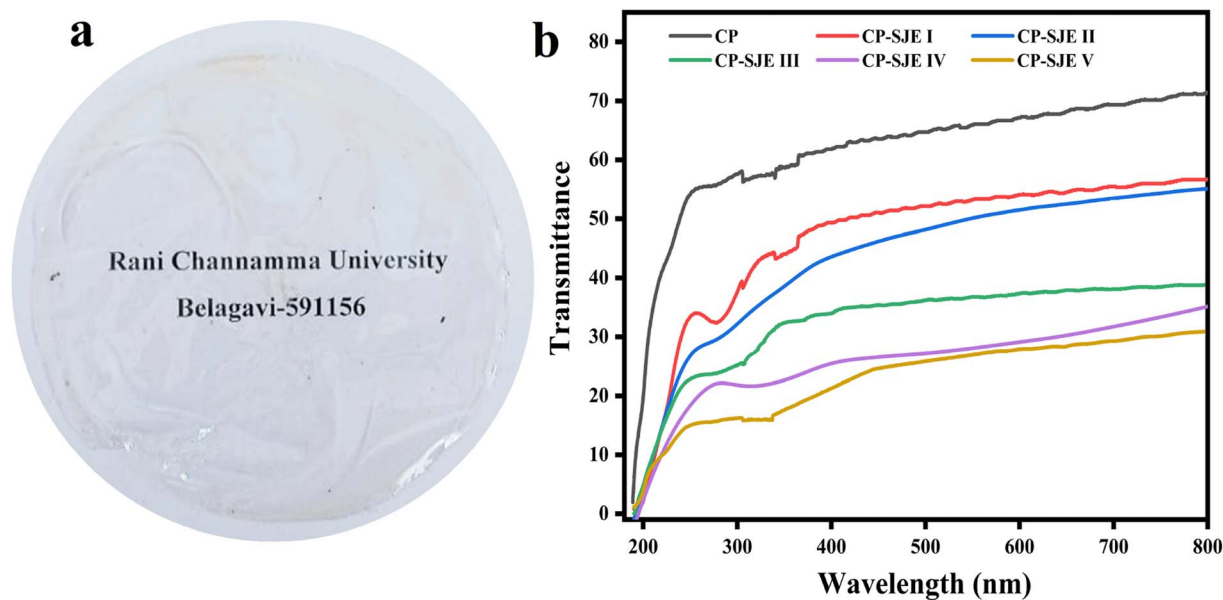


Fig. 5 Optical parameters; (a) visual appearance of CP-SJE-V film, (b) % transmittance of prepared films.

control CP and CP-SJE films, are summarized in Fig. 6. It is observed that the TS value of the CP film is 26.12 ± 0.83 MPa, and values for CP-SJE I, CP-SJE II, CP-SJE III, CP-SJE IV, and CP-SJE V films are 27.29 ± 0.91 MPa, 31.42 ± 0.96 MPa, 35.31 ± 1.00 MPa, 36.56 ± 0.79 MPa, and 38.68 ± 0.87 MPa, respectively. The EB value of the CP film is $30.51 \pm 0.29\%$, and values for CP-SJE I, CP-SJE II, CP-SJE III, CP-SJE IV, and CP-SJE V films are $28.11 \pm 1.07\%$, $27.14 \pm 0.93\%$, $26.09 \pm 0.83\%$, $24.19 \pm 1.03\%$, and $22.71 \pm 0.91\%$, respectively.

The YM value of the CP film was 0.3051 ± 0.7 GPa, and values for CP-SJE I, CP-SJE II, CP-SJE III, CP-SJE IV, and CP-SJE V films are 0.2821 ± 0.3 GPa, 0.2714 ± 0.6 GPa, 0.2609 ± 0.9 GPa, 0.2419 ± 0.2 GPa, and 0.2271 ± 0.5 GPa, respectively. However, it is also observed that as the concentration of the SJE on CP film increases, the tensile strength increases, and Young's modulus

and elongation break decreases ($P < 0.05$).^{43,44} This result is due to the abundant phenolic hydroxyl groups present in SJE that could interact with CS/PVA polymer through hydrogen bonds, thereby making films more compact (tensile strength).^{45,46} In addition, the incorporation of natural polyphenolic compounds could hinder chain-chain interactions of the CS/PVA matrix and thus greatly reduce the flexibility of CP-SJE films (elongation break).^{47,48}

Moisture content

Food packaging films should maintain certain moisture levels within the packaged products. Moisture content reflects the ability of packaging film to absorb moisture from a relatively high humid environment.⁴⁹ As shown in Table 2, SJE incorporation significantly reduced the moisture content of the CP-SJE films in comparison with CP film ($p < 0.05$). The MC values ranged from 26.74 to 39.18%. For control CP film, its high moisture content is caused by intermolecular interactions between water molecules and amino/hydroxyl groups alongside the molecular chain of CS/PVA. The incorporation of SJE could establish strong intermolecular interactions (hydrogen bonds) between anthocyanins and hydroxyl/amino groups of the CS/PVA chains, which greatly limited water-chitosan intermolecular interactions. Thus, the moisture contents in CP-SJE films decreased with the addition of SJE.

Water vapor transmission rate (WVTR)

The WVTR is a barrier parameter for the food packaging films to prevent the transfer of moisture from the outside atmosphere. The WVTR of control CP and CP-SJE films are shown in Table 2. The WVTR of the control CP film is 35.21 ± 0.13 g m⁻¹ h⁻¹. The WVTR values of CP-SJE films were lower in comparison to CP control film, and increasing SJE content in the prepared CP-SJE

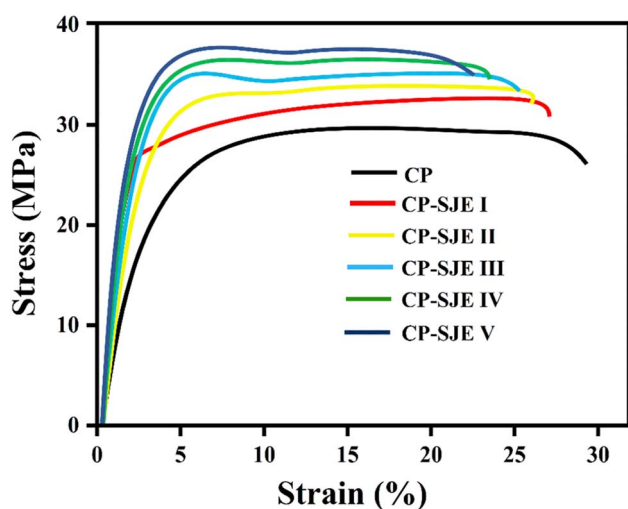


Fig. 6 Mechanical properties of control CP and CP-SJE films.



Table 2 Moisture capacity (MC), water vapor transmission rate (WVTR), water solubility (WS), and oxygen permeability (OP) of the prepared films^a

| Sample | MC (%) | WVTR (g m ⁻¹ h ⁻¹) | WS (%) | OP × 10 ⁻⁶ (cm ³ m ⁻¹ 24 h atm) |
|------------|----------------------------|---|----------------------------|--|
| CP | 39.18 ± 0.38 ^d | 35.21 ± 0.13 ^{ad} | 45.91 ± 1.31 ^a | 10.113 ± 1.315 ^{ad} |
| CP-SJE-I | 36.23 ± 0.19 ^c | 23.18 ± 0.16 ^{ab} | 46.36 ± 1.25 ^b | 9.109 ± 1 = 2.001 ^{ab} |
| CP-SJE-II | 34.92 ± 0.27 ^b | 22.31 ± 0.15 ^d | 48.42 ± 2.03 ^c | 8.215 ± 0.218 ^d |
| CP-SJE-III | 31.46 ± 0.35 ^d | 21.58 ± 0.1 ^c | 51.28 ± 1.45 ^d | 6.196 ± 1.853 ^c |
| CP-SJE-IV | 29.59 ± 0.52 ^{ab} | 20.67 ± 0.11 ^b | 53.53 ± 2.12 ^{ac} | 5.201 ± 1.791 ^b |
| CP-SJE-V | 26.74 ± 0.41 ^a | 18.39 ± 0.18 ^a | 56.41 ± 2.15 ^{ad} | 3.185 ± 0.532 ^a |

^a a–d Different letters represent statistical difference at $p < 0.05$, $n = 3$.

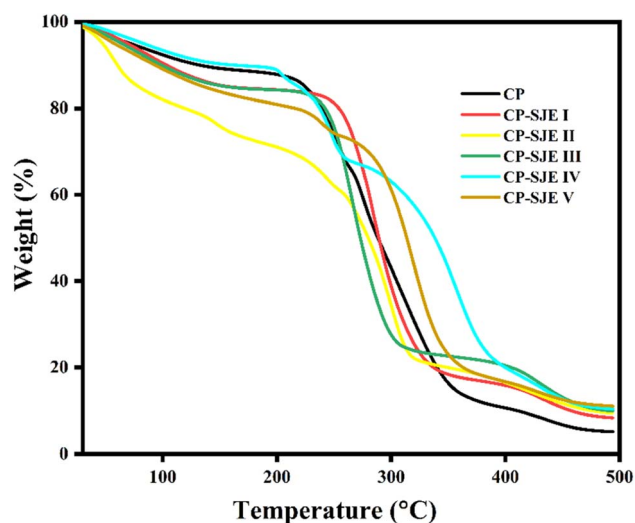


Fig. 7 TGA profile of control CP and CP-SJE films.

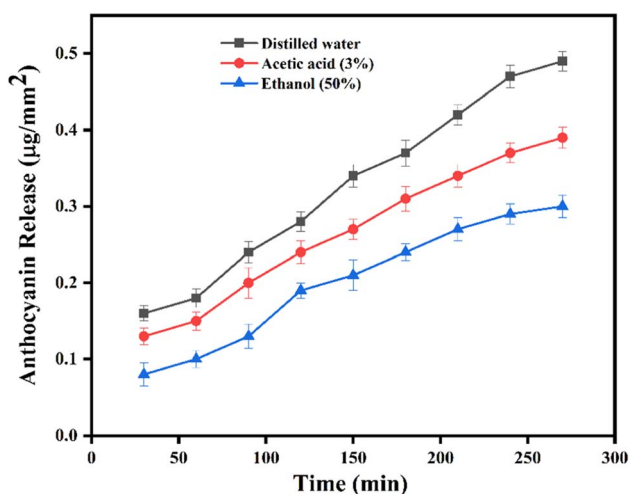


Fig. 8 Anthocyanin release into the food simulants.

composite caused a dramatic reduction in the WVTR values. With the addition of (0.33, 0.66, 1.00, 1.33, and 1.66 wt%) SJE, the WVTR value of CP-SJE films decreased in the order 23.18 ± 0.16 , 22.31 ± 0.15 , 21.58 ± 0.1 , 20.67 ± 0.11 , and 18.39 ± 0.18 , respectively (Table 2). The increase in SJE concentration reduces the WVTR values of CP-SJE films due to a number of factors,

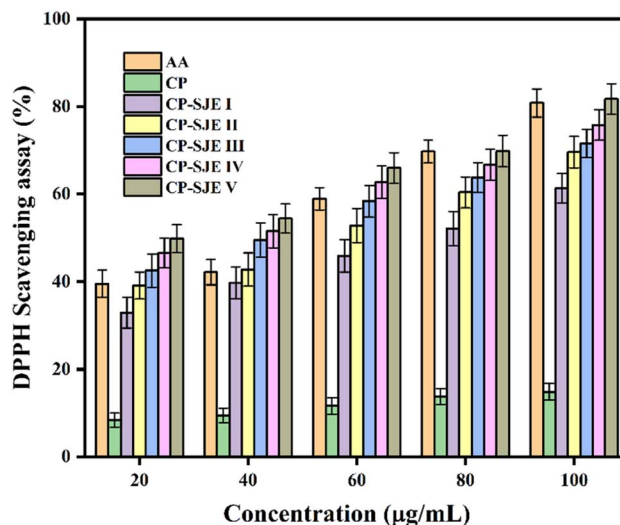
such as film density, surface structure, thickness, and hydrophilicity. Another important aspect that might obstruct the actual movement of water vapor diffusion is the compatibility and homogeneity of film.⁵⁰

Water solubility

Water solubility reflects the water resistance property of the prepared films. As summarized in Table 2, the control CP film showed the lowest water solubility ($45.91 \pm 1.31\%$), but the water solubility of CP-SJE films increased ($P \leq 0.05$) from $46.36 \pm 1.25\%$ to $56.41 \pm 2.15\%$ with increasing concentration of the SJE extract (Table 1). The enhanced water solubility is ascribed to the highly hydrophilic character of the anthocyanins present in the SJE. Similarly, increased water solubility was found in the corn and cassava starch-based films, and physicochemical characteristics are influenced by their starch content.⁵¹

Oxygen permeability (OP)

The oxygen barrier ability of the prepared films is an important parameter of food packaging materials. In general, the films with a low oxygen barrier ability are suitable to package fruits and vegetables, while the film with high oxygen barrier ability can protect food.³⁶ Table 2 summarizes the OP values obtained for CP and CP-SJE films. The OP value of the CP film is 10.113×10^{-6}

Fig. 9 Antioxidant profile of prepared control CP and CP-SJE films (mean ± SD, $n = 3$). *AA-ascorbic acid.

$\text{cm}^3 \text{m}^{-1} 24 \text{h atm}$, but lower OP values were observed for SJE loaded CP-SJE films than the control CP film. As the SJE content increased in polymer matrix, the OP value of CP-SJE composite films improved significantly ($p < 0.05$). The higher concentration of SJE loaded composite film (CP-SJE-V) exhibited the lowest OP value ($3.185 \times 10^{-6} \text{cc m}^{-1} 24 \text{h atm}$) among all other CP-SJE series films prepared (CP-SJE-I, CP-SJE-II, CP-SJE-III, and CP-SJE-IV). The reduction in the OP values of CP-SJE films caused by anthocyanin-rich extracts can be filled into the void volume in the film matrix and further establish intermolecular interactions with biopolymers resulting in a compact inner microstructure of the films.

Thermal properties of CP and CP-SJE films

TGA is a frequently used tool to analyze the thermal property of packaging films. TGA profiles of the prepared films are shown in Fig. 7, and the weight loss of the control CP and CP-SJE films appeared in three stages.⁵² The first stage appeared at 30–110 °C, the second at 111–260 °C, and the third stage was observed above 260 °C, which are due to the evaporation of moisture, intrinsic water in the film, and thermal decomposition of CS/PVA matrix and SJE. Notably, CP-SJE films showed more thermal stability than control CP film, which could be evidenced by the relatively slow degradation. In Fig. 7, it is revealed that SJE incorporation in CS/PVA matrix significantly increases the thermal stability of the CP-SJE films in comparison to the control CP film ($p < 0.05$). This property is due to the formation of strong intermolecular interactions between SJE and CP matrix, which requires more thermal energy to dissociate interactions. The control CP film showed 5.6% residue decomposition at 500 °C, while the weight percent remaining after major degradation at 500 °C for CP-SJE films was higher than the control CP. CP-SJE I, CP-SJE II, CP-SJE III, CP-SJE IV, and CP-SJE V had 7.9%, 8.2%, 9.2%, 10.03%, and 12.09% residue loss at 500 °C. According to this result, CP-SJE films have higher thermal stability than the control CP film.

Anthocyanins released from the films

The migration of a colorimetric indicator from smart packaging material is undesirable and not acceptable because it may lose its efficacy or discolor the food. For this reason, the rate of

anthocyanins released from the smart colorimetric films was determined using model food simulants such as water, ethanol, and acetic acid, which represented aqueous, alcoholic, and acidic food products, respectively.³⁷ Fig. 8 depicts the anthocyanin content released from the CP-SJE film profile. The results revealed that the release rate of anthocyanins in films was the fastest in distilled water ($0.49 \mu\text{g mm}^{-2}$), followed by 3% acetic acid ($0.37 \mu\text{g mm}^{-2}$) and 50% ethanol ($0.31 \mu\text{g mm}^{-2}$). This could be due to the high hydrophilicity of the CP-SJE films and the water-soluble behavior of the anthocyanins.

Antioxidant activity

The prepared films CP-SJE and control films were tested for their DPPH radical scavenging ability, and experimental data is appended in Fig. 9. It is observed that the control CP film showed much lower scavenging ability ($p < 0.05$).⁵³ The antioxidant ability of chitosan could be mainly attributed to the free radical scavenging ability of amino groups at the C-2 position of chitosan chains. In addition, the antioxidant mechanism of chitosan was also related to its metal ion chelating efficiency, which could prevent the initiation of lipid peroxidation. Notably, the antioxidant ability of CP-SJE films was closely related to the incorporated amount of SJE. For the CP-SJE films, their DPPH radical scavenging ability increased with increasing SJE contents ($p < 0.05$). These studies suggested the superior antioxidant ability of CP-SJE due to the functionality of polyphenolics present in the natural extract. Therefore, anthocyanin-rich CP-SJE films can be used to protect packaged food against oxidative damage. Table 3 represents some important previously reported anthocyanin-incorporated polymeric films compared with the present work, which revealed that the packaging films in the present work showed excellent antioxidant properties compared to other similar materials reported, probably due to the presence of a high concentration of active anthocyanins loaded on to the polymer matrix synergic effect.

Table 3 The literature comparison of maximum DPPH scavenging assay observed for different anthocyanin-incorporated polymeric films with present work

| Material composition | DPPH radical scavenging (%) | Reference |
|--|-----------------------------|---------------------|
| SFA/CaCl ₂ /BCE 1% | 32.96 | 40 |
| Car-LRM4.5 | 78.43 | 38 |
| Chitosan/AgNPs/PCE | 58.76 | 54 |
| $\kappa\text{C}/\text{HM40}/\text{Pm16}$ | 29.92 | 55 |
| Chitosan-BSSCE III | 59.01 | 52 |
| KCR-9 | 63.49 | 56 |
| CS-BRE III | 59.89 | 46 |
| CS-BEE III | 47.36 | 33 |
| Chitosan-PSPE III | 79.92 | 39 |
| CP-SJE-V | 81.72 | Present work |

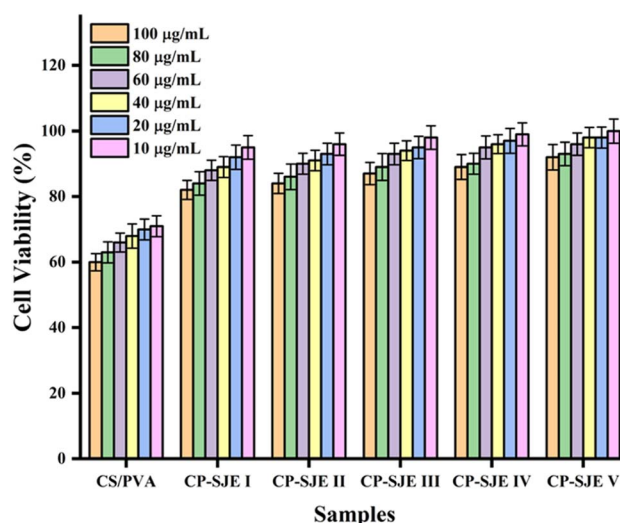


Fig. 10 Cell viability of prepared films against HEK293 cell line (mean \pm SD, $n = 3$).



Cell viability

The cell viability assay of chitosan-based film samples was examined by utilizing MTT assay [3-(4,5-dimethyl-2-thiazolyl)-2,5-diphenyl-2H-tetrazolium bromide] against HEK293 cell lines with concentrations of 10, 20, 40, 60, 80, and 100 $\mu\text{g mL}^{-1}$, after 24 h incubation at 37 °C (Fig. 10). All films exhibited maximum cell viability, and cells without treatment of anthocyanins were considered as control with cell viability more than 70%. As shown in Fig. 10, cell viability increased in response to the increase in the anthocyanin concentration and reached 99.75%. This indicates the biocompatibility of CS, PVA, and anthocyanin-containing composite films.^{57,58} The CP composite film with a higher concentration of SJE (CP-SJE V) showed higher cell viability. Altogether, these data suggest that CP-SJE films are non-toxic at a concentration of 10–100 $\mu\text{g mL}^{-1}$ as authenticated by experimental data on cell viability, which is greater than 90%.

Application of prepared films in chicken meat storage

The amount of nitrogenous constituents (ammonia, dimethyl, and trimethyl amine) in meat is measured using the TVBN (Total Volatile Basic Nitrogen) technique, which reveals the level of meat

freshness. In this study, pH-sensitive CP-SJE-V film is used to indicate the freshness of the chicken meat.³⁸ The change in the TVBN level of the chicken meat sample is shown in Fig. 11a. The initial TVB-N value for the sample is recorded as 7.82 mg/100 g. Samples exceeded the specified limit values after 46 h (20 mg/100 g), and after 60 h, TVB-N concentration increased to 40.19 mg/100 g. In the literature, generally, the acceptable TVB-N value is 20–30 mg/100 g for chicken meat according to Chinese Standard (GB 2733-2015).³⁸ This implied that the chicken meat sample could not be consumed after 46 h of processing. The pH of the food and its freshness are closely related. For instance, the pH indicator can detect significant pH changes that occur during the deterioration of the chicken flesh caused by the breakdown of protein and formation of amines. The prepared CP-SJE-V film was sealed within the package to monitor the freshness of the chicken meat and stored at ambient temperature (room temperature) for 60 h. The images showing the change in the film color starting fresh chicken meat and spoiled chicken meat are shown in Fig. 11b. The pH of the chicken meat was 6.5, 10.23, and 13.79 at 0, 30, and 60 h, respectively. Furthermore, it was noticed that CP-SJE-V film was light in color initially when the fresh chicken meat

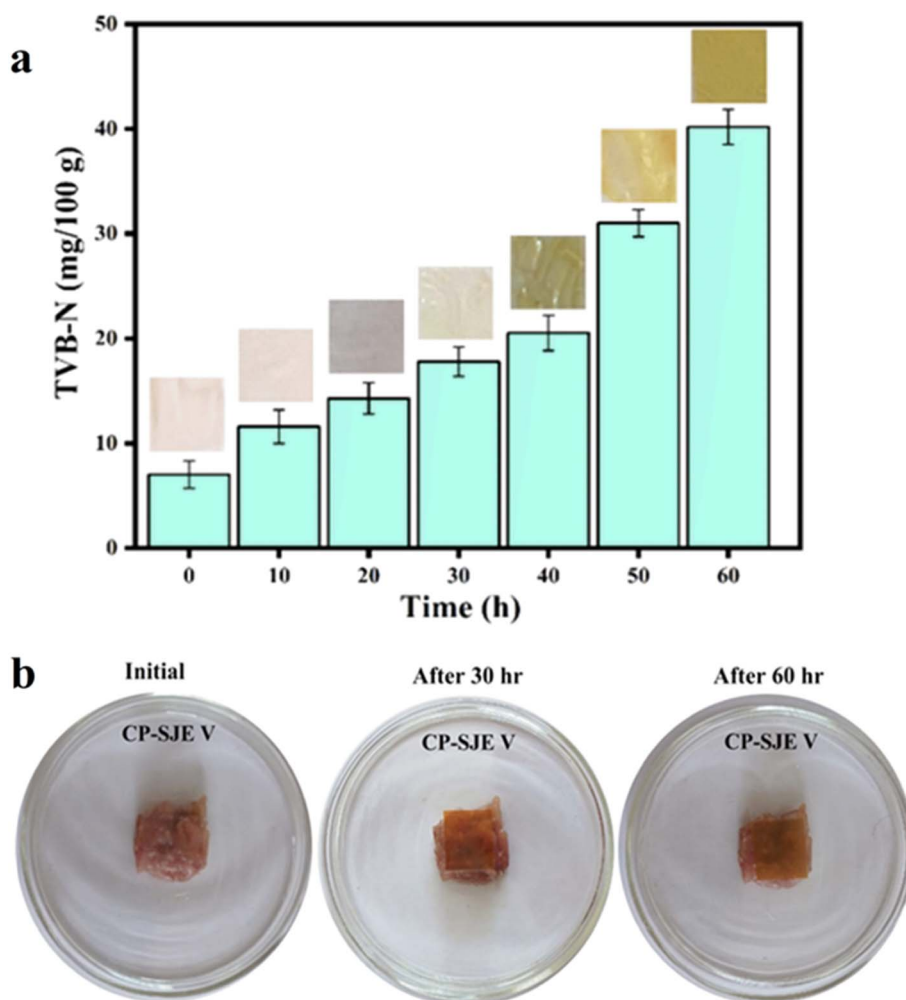


Fig. 11 (a) The change of TVB-N level of stored chicken meat from 0–60 h at rt (mean \pm SD, $n = 3$), (b) visualization of change in the freshness of the chicken meat during storage using CP-SJE-V film.



was packed, and after 30 h, the color of the CP-SJE-V film changed slightly yellowish, and finally, after 60 h, the packed film color (CP-SJE-V) changed to dark yellow. The color change of the CP-SJE-V film and the pH response of the films are in good agreement with each other. This result showed that the prepared CP-SJE films emerged as smart food packaging films for monitoring the freshness of the chicken meat.

Conclusion

The intelligent and active films were successfully prepared by incorporating anthocyanin-derived natural SJE into CP matrix. The CP-SJE films containing 1.66 wt% SJE exhibited excellent UV ray blocking ability (~63.75%), opacity (~58.06%), thickness (~32.05%), tensile strength (~32.47%), thermal stability (~53.68%), water solubility (~22.87%), and antioxidant activity (~71.31%) compared to the control CP film. The moisture retention capacity (~31.75%), oxygen permeability (~68.54%), water solubility (~22.87%), and water vapor transmission rate (~47.24%) were significantly enhanced with an increased SJE anthocyanin content. The pH-sensitive properties of the CP-SJE films were remarkably affected by the SJE content. The highest anthocyanin content film coded CP-SJE-V showed the most evident color change when applied to detect the freshness of the chicken meat examined, and the changed color can be easily watched by the naked eye. The rate of anthocyanins released from the film matrix into the food simulants is within the standard acceptable limits. All the CP-SJE films showed more than 90% cell viability. The CP-SJE films exhibited red color in acidic (pH = 1), while yellowish in basic (pH = 13). Hence, CP-SJE-V film emerged as the intelligent/active films category, providing consumers with real-time information about the quality and safety of the meat products, thereby reducing waste and time, and improving the health and sustainability of the food supply and packaging.

Abbreviations

| | |
|------------|--|
| AA | Ascorbic acid |
| ASTM | American society for testing and materials |
| ATR | Attenuated total reflection |
| CP | Chitosan/poly(vinyl alcohol) |
| CP-SJE | Chitosan/poly(vinyl alcohol)/SJE |
| CS | Chitosan |
| CP-SJE I | Chitosan/poly(vinyl alcohol)/SJE 0.33 wt% |
| CP-SJE II | Chitosan/poly(vinyl alcohol)/SJE 0.66 wt% |
| CP-SJE III | Chitosan/poly(vinyl alcohol)/SJE 1.00 wt% |
| CP-SJE IV | Chitosan/poly(vinyl alcohol)/SJE 1.33 wt% |
| CP-SJE V | Chitosan/poly(vinyl alcohol)/SJE 1.66 wt% |
| DDW | Double distilled water |
| DPPH | 2,2-Diphenyl-1-picrylhydrazyl |
| EB | Elongation at break |
| FT-IR | Fourier transform-infrared |
| MC | Moisture content |
| OP | Oxygen permeability |
| PVA | Poly(vinyl alcohol) |
| RH | Relative humidity |

| | |
|--------|---|
| SEM | Scanning electron microscope |
| SJE | <i>Stachytarpheta jamaicensis</i> extract |
| TGA | Thermogravimetric analysis |
| TPC | Total phenolic content |
| TS | Tensile strength |
| UTM | Universal testing machine |
| UV-vis | Ultraviolet-visible |
| WVP | Water vapor permeability |
| WVTR | Water vapor transmission rate |
| WS | Water solubility |
| YM | Young's modulus |

Data availability

All related data for this work is appended in the manuscript, and any detailed dataset required is available from the corresponding author on reasonable request.

Author contributions

Yamanappagouda Amaregouda: conceptualization; data curation; formal analysis; methodology; resources; software; roles: writing – original draft; writing – review & editing. Kantharaju Kamanna: investigation; supervision; designing work; validation; visualization; role: review & editing.

Conflicts of interest

There are no conflicts to declare.

Acknowledgements

Authors thank SERB-SURE, GoI, and RCUB for Interdisciplinary Minor Research Project for financial support. Authors are thankful to UGC for the award of Major Research Project and VGST, Govt. of Karnataka for the SMYSR award and RCUB-IRP-2022-23 for financial support to KK.

References

- 1 M. Vanderroost, P. Ragaert, F. Devlieghere and B. De Meulenaer, *Trends Food Sci. Technol.*, 2014, **39**, 47–62.
- 2 S. Sharma, S. Barkauskaite, A. K. Jaiswal and S. Jaiswal, *Food Chem.*, 2021, **343**, 128403.
- 3 G. Jiang, X. Hou, X. Zeng, C. Zhang, H. Wu, G. Shen, S. Li, Q. Luo, M. Li, X. Liu, A. Chen, Z. Wang and Z. Zhang, *Int. J. Biol. Macromol.*, 2020, **143**, 359–372.
- 4 F. Ebrahimi Tirtashi, M. Moradi, H. Tajik, M. Forough, P. Ezati and B. Kuswandi, *Int. J. Biol. Macromol.*, 2019, **136**, 920–926.
- 5 Q. Ma and L. Wang, *Sens. Actuators, B*, 2016, **235**, 401–407.
- 6 S. Kang, H. Wang, M. Guo, L. Zhang, M. Chen, S. Jiang, X. Li and S. Jiang, *J. Agric. Food Chem.*, 2018, **66**, 13268–13276.
- 7 J. G. de Oliveira Filho, A. R. C. Braga, B. R. de Oliveira, F. P. Gomes, V. L. Moreira, V. A. C. Pereira and M. B. Egea, *Food Res. Int.*, 2021, **142**, 110202.



- 8 R. R. Koshy, J. T. Koshy, S. K. Mary, S. Sadanandan, S. Jisha and L. A. Pothan, *Food Control*, 2021, **126**, 108039.
- 9 H. E. Khoo, A. Azlan, S. T. Tang and S. M. Lim, *Food Nutr. Res.*, 2017, **61**, 21.
- 10 E. Mohammadian, M. Alizadeh-Sani and S. M. Jafari, *Compr. Rev. Food Sci. Food Saf.*, 2020, **19**, 2885–2931.
- 11 P. M. Liew and Y. K. Yong, *Evidence-Based Complementary Altern. Med.*, 2016, **7**, 1–7.
- 12 J. P. Utami, S. Diana, R. Arifin, I. Taufiqurrahman, K. A. Nugraha, M. Widya and R. Y. Wardana, *J. Pharm. Pharmacogn. Res.*, 2022, **10**, 1087–1102.
- 13 D. M. Eskander, W. M. Aziz, M. I. Nassar and M. A. Hamed, *Biomarkers*, 2021, **26**, 606–616.
- 14 S. N. Vikasari, S. Wahyuningsih, A. B. Sutjiatmo and A. Razaq, *IOP Conf. Ser.: Earth Environ. Sci.*, 2021, **755**, 1–5.
- 15 A. M. Marpaung, I. Zhang and H. Sutanto, *IOP Conf. Ser.: Mater. Sci. Eng.*, 2019, **532**, 6.
- 16 A. Muxika, A. Etxabide, J. Uranga, P. Guerrero and K. de la Caba, *Int. J. Biol. Macromol.*, 2017, **105**, 1358–1368.
- 17 L. Racine, I. Texier and R. Auzély-Velty, *Polym. Int.*, 2017, **66**, 981–998.
- 18 Y. Amaregouda, K. Kamanna, T. Gasti and V. Kumbar, *J. Polym. Environ.*, 2022, **30**, 2559–2578.
- 19 Y. Amaregouda, T. Gasti and K. Kamanna, *IOP Conf. Ser.: Mater. Sci. Eng.*, 2022, **1221**, 012008.
- 20 Y. Amaregouda, K. Kamanna and T. Gasti, *J. Inorg. Organomet. Polym. Mater.*, 2022, **32**, 2040–2055.
- 21 Y. Amaregouda and K. Kamanna, *Indian Chem. Eng.*, 2022, **1–10**.
- 22 W. Lan, S. Wang, M. Chen, D. E. Sameen, K. J. Lee and Y. Liu, *Int. J. Biol. Macromol.*, 2020, **145**, 722–732.
- 23 M. Koosha and S. Hamedi, *Prog. Org. Coat.*, 2019, **127**, 338–347.
- 24 P. Terzioğlu, F. Güney, F. N. Parin, İ. Şen and S. Tuna, *Food Packag. Shelf Life*, 2021, **30**, 100742–100754.
- 25 Y. Amaregouda, K. Kamanna and T. Gasti, *Int. J. Biol. Macromol.*, 2022, **218**, 799–815.
- 26 V. A. Pereira, I. N. Q. de Arruda and R. Stefani, *Food Hydrocolloids*, 2015, **43**, 180–188.
- 27 I. Păușescu, A. Todea, V. Badea, F. Peter, M. Medeleanu, I. Ledeti, G. Vlase and T. Vlase, *J. Therm. Anal. Calorim.*, 2020, **141**, 999–1008.
- 28 S. S. Narasagoudr, V. G. Hegde, R. B. Chougale, S. P. Masti, S. Vootla and R. B. Malabadi, *Food Hydrocolloids*, 2020, **109**, 106096.
- 29 N. A. Hidayati, M. W. Wijaya, V. P. Bintoro, S. Mulyani and Y. Pratama, *Food Res.*, 2021, **5**, 307–314.
- 30 E. Genskowsky, L. A. Puente, J. A. Pérez-Álvarez, J. Fernandez-Lopez, L. A. Muñoz and M. Viuda-Martos, *LWT-Food Sci. Technol.*, 2015, **64**, 1057–1062.
- 31 K. Chayavanich, P. Thiraphibundet and A. Imyim, *Spectrochim. Acta, Part A*, 2020, **226**, 117601.
- 32 T. Gasti, S. Dixit, V. D. Hiremani, R. B. Chougale, S. P. Masti, S. K. Vootla and B. S. Mudigoudra, *Carbohydr. Polym.*, 2022, **277**, 118866.
- 33 H. Yong, X. Wang, X. Zhang, Y. Liu, Y. Qin and J. Liu, *Food Hydrocolloids*, 2019, **94**, 93–104.
- 34 M. S. Sarwar, M. B. K. Niazi, Z. Jahan, T. Ahmad and A. Hussain, *Carbohydr. Polym.*, 2018, **184**, 453–464.
- 35 S. Huang, Y. Xiong, Y. Zou, Q. Dong, F. Ding, X. Liu and H. Li, *Food Hydrocolloids*, 2019, **90**, 198–205.
- 36 S. Yadav, G. K. Mehrotra, P. Bhartiya, A. Singh and P. K. Dutta, *Carbohydr. Polym.*, 2020, **227**, 115348.
- 37 Y. C. Wei, C. H. Cheng, Y. C. Ho, M. L. Tsai and F. L. Mi, *Food Hydrocolloids*, 2017, **69**, 491–502.
- 38 J. Liu, H. Wang, M. Guo, L. Li, M. Chen, S. Jiang, X. Li and S. Jiang, *Food Hydrocolloids*, 2019, **94**, 1–10.
- 39 H. Yong, X. Wang, R. Bai, Z. Miao, X. Zhang and J. Liu, *Food Hydrocolloids*, 2019, **90**, 216–224.
- 40 S. Kim, S. K. Baek and K. Bin Song, *Food Packag. Shelf Life*, 2018, **18**, 157–163.
- 41 S. Kang, H. Wang, L. Xia, M. Chen, L. Li, J. Cheng, X. Li and S. Jiang, *Carbohydr. Polym.*, 2020, **229**, 115402.
- 42 S. Wu, W. Wang, K. Yan, F. Ding, X. Shi, H. Deng and Y. Du, *Carbohydr. Polym.*, 2018, **186**, 236–242.
- 43 E. Jamróz, P. Kulawik, P. Guzik and I. Duda, *Food Hydrocolloids*, 2019, **97**, 105211.
- 44 M. Koosha and S. Hamedi, *Prog. Org. Coat.*, 2019, **127**, 338–347.
- 45 Y. Liu, Y. Qin, R. Bai, X. Zhang, L. Yuan and J. Liu, *Int. J. Biol. Macromol.*, 2019, **134**, 993–1001.
- 46 H. Yong, J. Liu, Y. Qin, R. Bai, X. Zhang and J. Liu, *Int. J. Biol. Macromol.*, 2019, **137**, 307–316.
- 47 X. Zhang, Y. Liu, H. Yong, Y. Qin, J. Liu and J. Liu, *Food Hydrocolloids*, 2019, **94**, 80–92.
- 48 J. Sun, H. Jiang, H. Wu, C. Tong, J. Pang and C. Wu, *Food Hydrocolloids*, 2020, **107**, 105942.
- 49 M. Kurek, L. Hlupić, I. Elez Garofulić, E. Descours, M. Ščetar and K. Galić, *Food Packag. Shelf Life*, 2019, **20**, 100315–100324.
- 50 T. Gasti, S. Dixit, O. J. D'souza, V. D. Hiremani, S. K. Vootla, S. P. Masti, R. B. Chougale and R. B. Malabadi, *Int. J. Biol. Macromol.*, 2021, **187**, 451–461.
- 51 C. L. Luchese, J. C. Spada and I. C. Tessaro, *Ind. Crops Prod.*, 2017, **109**, 619–626.
- 52 X. Wang, H. Yong, L. Gao, L. Li, M. Jin and J. Liu, *Food Hydrocolloids*, 2019, **89**, 56–66.
- 53 M. Mushtaq, A. Gani, A. Gani, H. A. Punoo and F. A. Masoodi, *Innovative Food Sci. Emerging Technol.*, 2018, **48**, 25–32.
- 54 Y. Qin, Y. Liu, L. Yuan, H. Yong and J. Liu, *Food Hydrocolloids*, 2019, **96**, 102–111.
- 55 G. Sun, W. Chi, C. Zhang, S. Xu, J. Li and L. Wang, *Food Hydrocolloids*, 2019, **94**, 345–353.
- 56 C. Wu, Y. Li, J. Sun, Y. Lu, C. Tong, L. Wang, Z. Yan and J. Pang, *Food Hydrocolloids*, 2020, **98**, 105245.
- 57 M. Cheng, X. Yan, Y. Cui, M. Han, Y. Wang, J. Wang, R. Zhang and X. Wang, *Polymers*, 2022, **14**, 1214–1228.
- 58 N. Karimi, A. Alizadeh, H. Almasi and S. Hanifian, *LWT-Food Sci. Technol.*, 2020, **121**, 108978.

